Journal of Power Sources 186 (2009) 80–88

Contents lists available at ScienceDirect

Journal of Power Sources

journal homepage: www.elsevier.com/locate/jpowsour

Experimental and theoretical investigations on a proton exchange membrane fuel cell starting up at subzero temperatures

E. Pinton*, Y. Fourneron, S. Rosini, L. Antoni

Commissariat a l'Energie Atomique (CEA/LITEN), LITEN/DTH/LPAC, 17 rue des Martyrs, 38 054 Grenoble Cedex 9, France

ARTICLE INFO

Article history:
Received 29 May 2008
Received in revised form 25 August 2008
Accepted 10 September 2008
Available online 25 September 2008

Keywords:
PEMFC
Cold start
Experimental results
Phenomenological interpretation
Operating parameter effects
Ageing

ABSTRACT

Ice/frost formation in a proton exchange membrane fuel cell (PEMFC) operating under subzero temperatures can lead to its shutdown during start up. Isothermal potentiostatic and galvanostatic tests were performed on 220 cm^2 single cells under a wide range of operating conditions in order to investigate the "cold start" behaviour. Different parameters have been investigated: the initial water contained in the membrane, the operating voltage, the cell temperature and current. An optimal wetting level of the fuel cell (FC) core for which cumulated heat generated by the electrochemical reaction is maximal, has been observed. Water management analysis from the membrane coupled with cell resistance measurement allowed to formulate a phenomenological interpretation of the overall FC performance evolution. FC starving is not only due to ice formation in the cathode layer pores, thus hindering oxygen transport. It is also due to ice formation in active reaction sites increasing the electrical resistance of the cell. Both factors dramatically reduce FC performance under load. The relative balance of each effect has been assessed. After each shutdown and start up at subfreezing temperature, a polarization curve at rated conditions was carried out to quantify the FC performance degradation. Performances reduce less than 1% per cold start at rated current density.

1. Introduction

Proton exchange membrane fuel cell (PEMFC) is one of the most promising technologies to produce clean electricity with only water as exhaust product. However, water management gives rise to technical complications, especially for automotive application in winter conditions. It is commonly described in the literature that the fuel cell (FC) shutdown is due to ice formed in the cathode catalyst layer (CCL) by the oxygen reduction reaction (ORR), thus hindering oxygen transport. This ice may entail structural damages to the membrane electrode assembly (MEA). Cold start is supposed to succeed when the cell temperature rises above the freezing point of the water inside the catalyst layer (CL). Even if substantial research efforts have been made for the last 4 years, the effects of start up at subzero temperature remain scarce [1–8].

To maintain stable cell performances below the freezing point, Hishinuma et al. [1] proposed to adjust the current densities and the gas flow rates to balance produced and removed water. However, below −5 °C additional heat sources are necessary to start the fuel cell.

In order to examine basic cold start behaviours of PEMFCs, Oszcipok et al. [2] conducted isothermal potentiostatic cold start measurements of a single cell. They indicate that, if the membrane is initially dried, the produced water is first absorbed by the polymer. Then once the membrane humidity reaches its maximum, the produced water is thrown out in the CCL and in the gas diffusion layer (GDL) and freezes. Ice formation would subsequently lead to strong current density decay and cell degradation. Mathematic fitting curve and statistic regression analyses have also been carried out, and it has been showed that dried membrane and high gas flow rates are beneficial for the PEMFC cold start operations. Compared with [2], Oszcipok et al. [3] present additional tests performed on a six cells stack with an active area of 30 cm^2. Bipolar plates are made of graphite compound. The stack is located in a climatic chamber. For an initial FC temperature of −10 °C, self-starting succeeded in less than 4 min by gradually increasing of the imposed current. However, this time duration remains again too long for automotive application. Self-starting did not succeed for an initial temperature of −20 °C. The authors also deduced from this experiment that for a successful cold start up the membrane should not be too dry.

Cold start behaviour and effect of subzero temperatures on FC performance were studied by Yan et al. [4]. A 25-cm^2 single cell was housed in an environmental chamber. Cold start measurements showed that the cell was able to start operation at −5 °C without irreversible performance loss when the cell was initially

* Corresponding author. Tel.: +33 4 76 29 48 23; fax: +33 4 38 78 94 63.
E-mail address: eric.pinton@cea.fr (E. Pinton).

0378-7753/$ – see front matter © 2008 Elsevier B.V. All rights reserved.
doi:10.1016/j.jpowsour.2008.09.056

Nomenclature

CL	catalyst layer
CCL	cathode catalyst layer
F	Faraday number (96 487 C mol^{-1})
FC	fuel cell
GDL	gas diffusion layer
i	current density (A cm^{-2})
I	current (A)
MEA	membrane electrode assembly
MPL	microporous layer
N_{H_2O}	amount of produced water (mol)
ORR	oxygen reduction reaction
P	pressure (barA)
PEMFC	proton exchange membrane fuel cell
Qth	cumulated heat density generated by the electrochemical reaction (J cm^{-2})
R	resistance (Ω cm^2)
RH	relative humidity (%)
R_{cell}	cell resistance (Ω cm^2)
R_{memb}	membrane resistance (Ω cm^2)
$R_{U_{max}}$	minimal cell resistance at U_{max} (Ω cm^2)
$R_{20\,°C}$	cell resistance at 20 °C (Ω cm^2)
SEM	scanning electron microscopy
St	stoichiometry
t	time (s)
t_{memb}	membrane thickness (m)
T	temperature (°C)
U	cell voltage (V)
U_{max}	maximal voltage (V)

Greek symbols

$\Delta\eta_{Electrodes}$	change in electrodes activation and diffusion overpotential (V)
ΔU_Ω	change in ohmic potential (V)
λ	water content of the membrane (ratio of the water molecule to the number of charge sites)
σ_{memb}	proton conductivity of the membrane (S m^{-1})

dry. However, irreversible performance losses were found if the cell temperature at the cathode side falls below −5 °C during operation. Significant damage to the MEA and backing layer was observed with a scanning electron microscopy (SEM), including catalyst layer delimitation from both the membrane and the GDL and cracks in the membrane.

Tajiri et al. [5,6] describe an experimental study on the effects of operating and design parameters on PEMFC cold start capability. A newly developed isothermal cold start protocol is used to explore the basic physics of cold start. The influence of purge methods prior to cold start, start up temperature, current density and the membrane thickness was investigated. The results and the analysis are in accordance with Oszcipok et al. [2].

Ge and Wang [7] explore experimentally the fundamental characteristics of a PEMFC during subzero start up, which encompasses gas purge, cool down, start up from a subfreezing temperature, and finally warm up. In addition to the temperature, high frequency resistance and voltage measurements have been carried out. It came out that gas purge and subfreezing temperature are key parameters to ensure self-start of the FC.

Recently, a cyclic voltammetry technique has been used by Ge and Wang [8] to investigate the effect of ice formation in the CCL on electrochemically active Pt area during and post-subzero start up. The active Pt area is found to decrease after cold start. This loss is believed to be caused by the formation of ice sheets between Pt particles and ionomers in the CCL. After start up from a subzero temperature and warm up to 25 °C with all ice in the CL melted, the cell remains subject to Pt area loss, but this loss at 25 °C is substantially reduced. This remaining Pt area loss can be largely recovered by operating the cell at 70 °C and high current density for an extended period of time. This indicates that liquid water trapped between Pt particles and ionomers can be removed at high elevated temperature and with high reaction heat. However, permanent CL degradation, due to structural alteration of the CCL induced by the presence of ice, increases gradually with the cold start cycle number, at levels ranging from 1 to 3% per cold start. No active Pt area loss in the anode CL was found. This can be explained by the fact that no water is produced electrochemically at the anode.

MEA durability from freeze/thaw cycles without water production was studied [8–12]. It is generally observed that repetitive freezing and melting of water of a fully hydrated cell damages MEA structure and cell performance. However, according to Hou et al. [12] and Guo and Qi [13], no consequences are noticed if dry gases are previously used to remove some water from the cell.

Using a micro-X-ray beam, the structure of a water swollen Nafion® membrane, alone or in a MEA designed for FC, was studied by Pineri et al. [14] upon cooling down to −70 °C. By scanning the membranes along their thicknesses, the water sorption–desorption process was investigated as a function of cooling/heating stages. From the scattering curves, it was deduced that the state of the water at a subzero temperature is glassy/liquid inside the membrane. Ice crystals are only observed outside it. In the case of the MEA, this growth can be destructive since this formation is localised inside the active layers.

CEA has developed in collaboration with PSA Peugeot Citroën a specific compact PEMFC stack (GENEPAC) with an operating temperature target at around 80 °C. However, cold start behaviour and capability at subzero temperatures have to be assessed with this technology which is relatively different from standard laboratory FC design. Tests were performed on 220 cm^2 single cells made of metallic monopolar plates under a wide range of operating conditions in order to define the effect of some critical parameters. These parameters are the initial water contained in the membrane, the imposed voltage or current density and the cell temperature. The investigated complete sequence of PEMFC cold start includes FC operating at rated conditions, dry purge, cool down, cold start and shut down. This paper deals with the interpretation and the analysis of the experimental results. A fundamental mechanism governing the electrochemical and cell resistance during cold start is proposed. This should finally help to define optimal start up and shutdown strategy at freezing temperature in terms of time compatible with automotive application, consumed energy (self-starting if possible without additional heat sources) and cell damages.

2. Experimental

2.1. Experimental set-up

Experiments were carried out on a single cell with an active area of 220 cm^2. The cell consists of a commercial MEA with GDL, microporous layer (MPL) and catalyst-coated membrane (Nafion® base). The MEA is in contact with two monopolar plates made of thin metallic sheet and having serpentine flow fields on anode and cathode sides. A cooling fluid circulates inside the metallic plate in order to control cell temperature. A specific short stack test station has been developed in house for cold start tests (Fig. 1). It comprises sub-systems to provide fuel and oxidant to the stack (air and

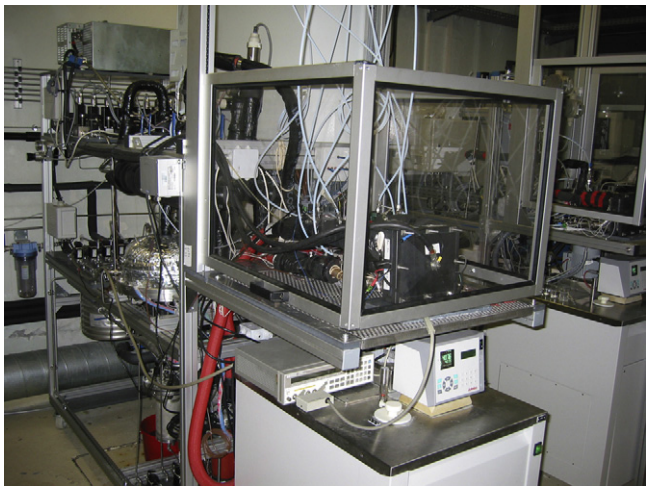

Fig. 1. Photo of the experimental set-up.

H_2 flow rates, pressure, temperature, wet or dry gases), an electronic load for dissipating the delivered electrical energy of the FC, and a thermo-control sub-system to regulate temperature of the cell core from −20 to 100 °C. Because of the very thin monopolar metallic plates it is not possible to measure the temperature of the FC core. It is supposed to be the temperature measurement of coolant fluid at the FC outlet. This hypothesis is quite good because the coolant flow is very high (the coolant within the cell is changed 300 times per minute) and the internal heat exchanges are very efficient. While recording voltage–time curves during constant current density start up or recording current density–time curves during constant voltage start up, the ohmic cell resistance is measured by an Agilent milliohm meter of AC current at 1 kHz.

2.2. Testing procedure

The principle is to perform several cold starts by only varying one operating condition at each start up. The goal is to highlight the impact and the sensitivity of the key parameters influencing the behaviour of a FC starting at negative temperatures. These parameters are

- water content of the membrane,
- voltage or current density depending on the mode of load control,
- cell temperature can be:
  - kept constant,
  - controlled by upward or downward ramps,
  - free.

A cold start consists of operating a FC at low temperature in potentiostatic or galvanostatic mode with dry gases and controlled pressure, stoichiometry, temperature and initial humidity. The initial hydric rate inside the FC core is represented by the ohmic cell resistance "$R_{20\,°C}$" (measurement of the real part of impedance at 1 kHz and at the drying temperature of 20 °C). Actually, for a given temperature above 0 °C, the cell resistance represents mainly the membrane resistance which is strongly dependent on its water content.

The baseline conditions generally applied at low temperature are

- Cell voltage: $U = 0.5$ V.
- Cell temperature: $T = -10$ °C.
- Cell resistance: $R_{20\,°C} = 2.5\ m\Omega$ ($0.55\ \Omega\ cm^2$).
- H_2 pressure: $P_{H_2} = 1.5$ barA.
- O_2 pressure: $P_{air} = 1.5$ barA.
- H_2 stoichiometry $St_{H_2} = 1.5$ (flow rate controlled by the stoichiometry for a current density above $0.045\ A\ cm^{-2}$, otherwise it is fixed at $6\ NL\ h^{-1}$).
- O_2 stoichiometry $St_{O_2} = 2$ (air flow rate controlled by the stoichiometry for a current density above $0.045\ A\ cm^{-2}$, otherwise it is fixed at $20\ NL\ h^{-1}$).

The reference procedure applied is the following:

1. FC assembly with a new MEA and conditioning.
2. FC operating at rated conditions (80 °C) with wet gases (RH = 50%) for at least 30 min and until the stabilization of the cell voltage.
3. FC polarization curve (baseline of FC performance).
4. FC cooling from 80 to 20 °C.
5. FC drying with dry nitrogen until it reaches the testing resistance $R_{20\,°C}$. Then N_2 flow rate is slowly decreased while keeping $R_{20\,°C}$ constant and until the flow is zero. $R_{20\,°C}$ remains stable after the end of this drying method. The appendix presents a method to assess the water content of the membrane as a function of $R_{20\,°C}$.
6. FC cooling down to the testing temperature (water content in the membrane is assumed to be constant because the amount of vapour inside channels capable of condensing is very small in comparison with).
7. FC start up
   (A) mainly in potentiostatic mode where voltage is kept constant until the current density reaches about $0.023\ A\ cm^{-2}$ (partial starving) or less than $0.0045\ A\ cm^{-2}$ (nearly complete starving),
   (B) or in galvanostatic mode where current density is kept constant until the voltage drops below the cut off voltage of 0.2 V.
8. Start again from step 2 if a new value of testing parameter has to be tested.
9. FC operating at rated conditions followed by a polarization curve (baseline of FC performances).
10. End of the test series of the parameter investigated.

3. Results and discussion

3.1. FC general behaviour during start up and shut down

Fig. 2a shows the general evolution of the current density and the cell resistance with time for typical potentiostatic cold start. Fig. 2b displays additionally the shutdown period. Four characteristic times are distinguished:

- t_0: the electronic load is connected.
- t_0–t_1: the current density increases and the cell resistance decreases.
- t_1: the current density reaches its maximal value and the cell resistance its minimal value.
- t_1–t_2: the current density drops and the cell resistance rises.
- t_2: the electronic load is disconnected and gas flows are cut off.
- t_2–t_3: the cell resistance decreases up to tend toward an equilibrium.
- t_3: the minimal cell resistance is reached.

Water management analysis from the membrane coupled with cell resistance measurement allowed to formulate a phenomenological interpretation of the overall FC electrochemical response during

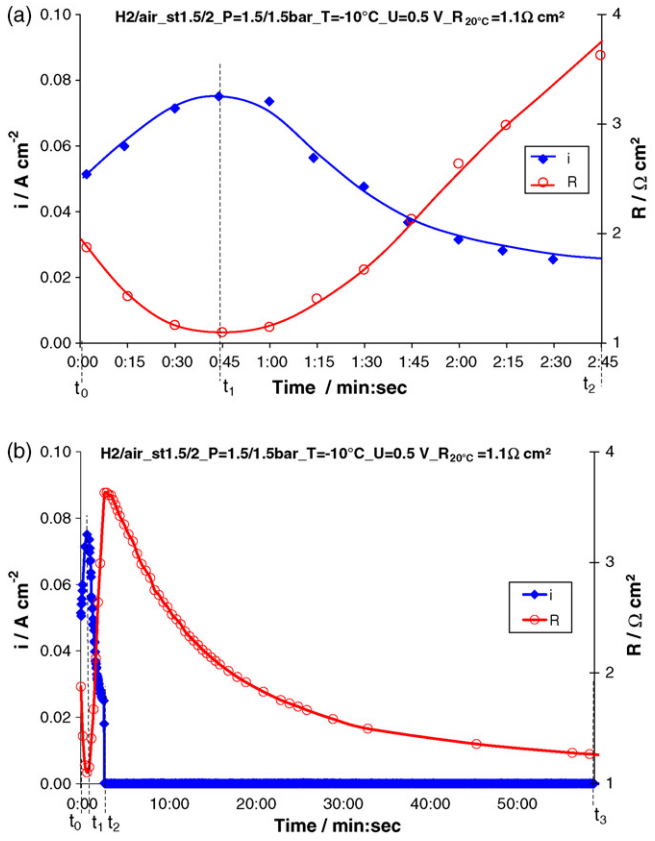

Fig. 2. (a) General evolution of current density and cell resistance during a potentiostatic cold start and (b) General evolution of current density and cell resistance during a short potentiostatic cold start and during the shutdown period.

cold start. This interpretation is supported by the work in Refs. [1–8].

When the electronic load is connected (t_0), water produced from the ORR is absorbed by the previously dried membrane, leading to a decrease of its resistance value. A water gradient must exist inside the membrane because of the competition between the electro-osmotic drag and the water diffusion. This gradient could be significant as the diffusion coefficient of water in the membrane decreases substantially with water content and temperature. The current density reaches a maximal value when the resistance is minimal (t_1). At this time, the membrane at the cathode side is almost saturated and additional produced water cannot be totally absorbed and thus begins to freeze in the CCL. The resistance increase observed after this point (t_1–t_2) could be explained by the presence of ice inducing an additional electrical contact resistance whereas the membrane conductivity remains practically stable or decreases very slightly. Afterwards, all produced water freezes inside the cathode catalyst active area and the resistance rises quickly. According to the measured resistance evolution, it can be concluded that, at least for the investigated MEA type, FC starving during cold start is not only due to pores plugged by ice/frost, thus hindering oxygen transport and reducing the active electrochemical area. It also derives from ice formation, leading to an increase in the electrical contact resistances. It is proposed that ice formed inside the CCL does not locate at the same place during the cooling step and during cold start step. Actually, during the cooling step of a fully hydrated MEA (no drying) which previously operated at rated conditions, no cell resistance jump is observed (Fig. 3), whereas it increases sharply during the cold start starving stage once the membrane content at the cathode side is saturated (Fig. 2b). Thus,

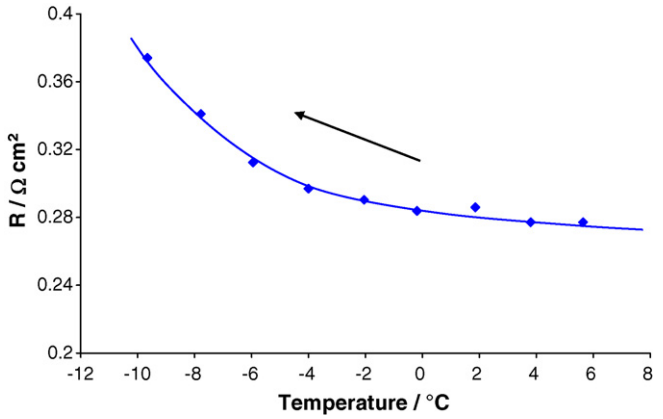

Fig. 3. Evolution of the cell resistance of a fully hydrated MEA (no drying) during the cooling step.

ice formed in a wet MEA due to FC cooling without operation would locate only in the hydrophilic pores. During starving phases, ice would not only locate in the pores of the CCL, but also at the interfaces of particle agglomerates of ionic and electronic conductors inside the CCL. This interpretation agrees in part with the ones of Ge and Wang [8] and Oszcipok et al. [15]. Ge and Wang [8] proposed that ice would locate between Pt particles and the ionomer. Oszcipok et al. [15] observed experimentally a small step contact resistance increase when starving occurs. They suggest that this step could be explained by contact resistance increase between cell layers, while membrane resistance is continuously decreasing.

Once the load is disconnected (for a current density of about 0.023 A cm^{-2}) and the gas flows cut off (t_2), the cell resistance decreases up to reach a constant value. The membrane at the cathode side is saturated because it is in equilibrium with frozen water and water vapour inside the pores and the interstice of CCL. This frozen water sublimates to maintain the thermodynamic equilibrium at the membrane interface because of water content gradient remaining in the membrane thickness. The sublimated vapour is thereby absorbed by the membrane by water diffusion from the cathode to the anode side. Thus ice content and therefore the contact resistances decrease. This process continues until homogeneous water saturation is obtained inside the membrane thickness.

Fig. 4 summarizes the supposed water content "λ" time evolution in the membrane thickness and the supposed membrane and contact resistances time evolution.

The previous interpretation of the cell resistance behaviour during the shut down period is reinforced by a specific test. The FC operates during a very long time, nearly 40 min (see Fig. 5), and at very low current ($i < 0.0045$ A cm^{-2}). In this case water transport by electro-osmotic drag is very weak. The membrane at the anode side has enough time to rehydrate itself and to reach saturated water content. Consequently, ice does not sublimate and cannot be absorbed by the membrane. Thus, the cell resistance remains stable during the shut down period as shown in Fig. 5 (time > t_2).

3.2. Effect of the initial humidity level

Fig. 6 presents the effect of the FC drying level on potentiostatic cold starts. For the cell without drying, starving is immediate, whereas a dried cell can operate during a few tens of seconds before starving. The higher is the initial level of drying, the longer is the starving priming. Actually, with an initial drying level up to $R_{20\,^\circ C} = 0.55\ \Omega\ cm^2$, more water can be absorbed by the membrane before water saturation is reached. Then, for drying levels higher than $R_{20\,^\circ C} = 0.55\ \Omega\ cm^2$, current density is significantly reduced

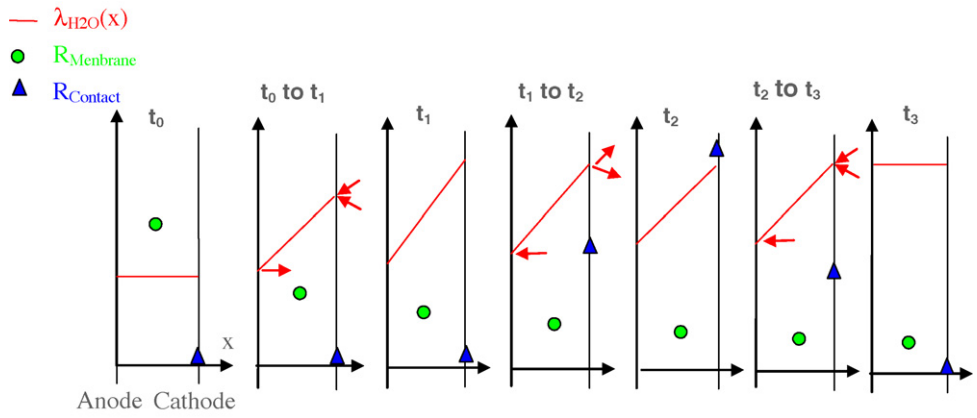

Fig. 4. Evolution of water content and resistances during a potentiostatic cold start.

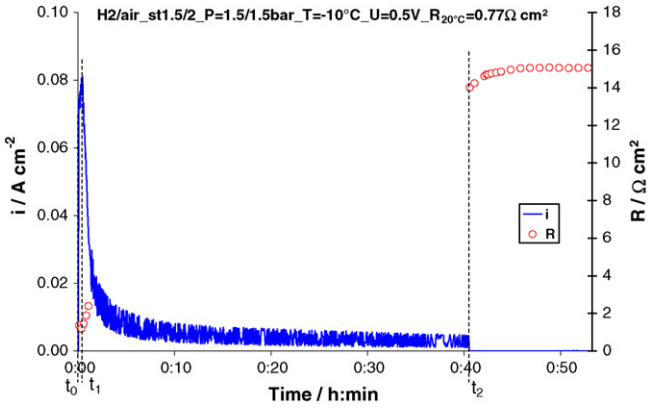

Fig. 5. General evolution of current density and cell resistance during a long potentiostatic cold start and during the shutdown period.

mainly because of a lower proton conductivity of the membrane. Thus more time is needed to saturate the membrane. Nevertheless, an optimal wetting level appears between a non-dried and a strongly dried membrane, where cumulated heat density generated by the electrochemical reaction "Qth" is maximal, at $R_{20\,^\circ C} \sim 0.55\,\Omega\,cm^2$ (see Fig. 7).

$$Qth(t) = \int_0^t (E_{th} - U_{cell}) i\,dt \quad (1)$$

where "*E*th" is the thermodynamic voltage (*E*th ~ 1.252 V for H_2/O_2 reaction giving H_2O vapour at normal conditions). Actually, there are two opposite phenomena. Initial drying reduces cold start performance when the FC operates before starving (*Q*th ↓), but at the same time it allows to operate longer (*Q*th ↑). Thus, in order to obtain a maximal heat density generation to allow to self-starting without additional heat sources, FC will have to be dried at an optimal value. This conclusion is supported by Oszcipok et al. [3] who suggest that for a successful cold start up the membrane should not be too dry.

3.3. Effect of imposed voltages

Fig. 8 displays the voltage effect on potentiostatic cold starts. A decrease in voltage leads to shorter FC operation before starving as more water is produced at higher current densities. Therefore, less time is needed to saturate the membrane with a voltage decrease. To take the maximum benefit from the corresponding produced reaction heat, starting at low voltage ($0.3 < U_{cell} < 0.5$ V) and high current density seems preferable.

3.4. Effect of temperature ramps

Experimental results displayed in Fig. 9 are the continuity of a long cold start test as shown previously in Fig. 5. Once the electronic load is reconnected, upward and downward temperature ramps have been imposed with a rate about 2 °C min^{-1}. A steep transition of the cell resistance and the cell current are observed at the

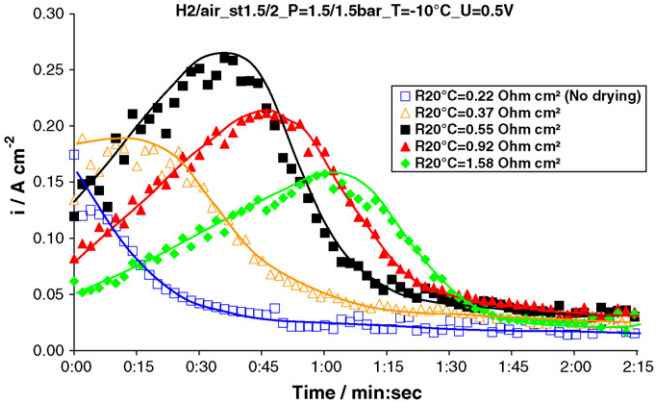

Fig. 6. Time evolution of current density during cold starts at different initial drying levels.

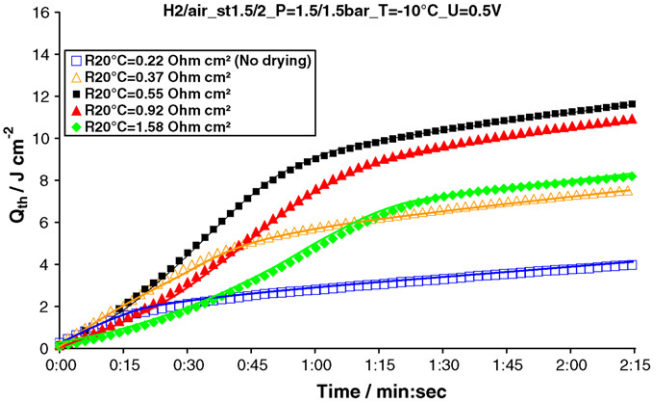

Fig. 7. Time evolution of cumulated heat density generation during cold starts at different initial drying levels.

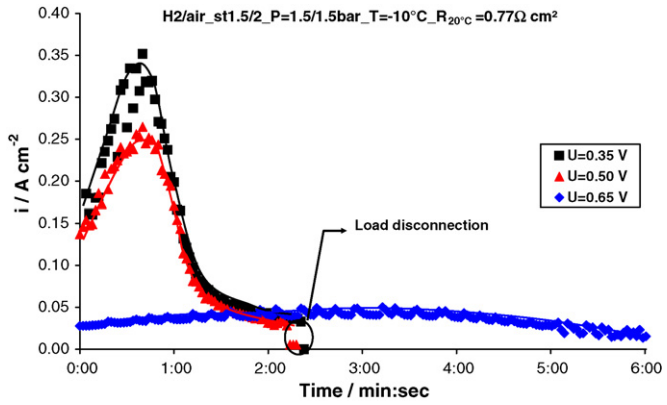

Fig. 8. Time evolution of current density during cold starts at different imposed voltages.

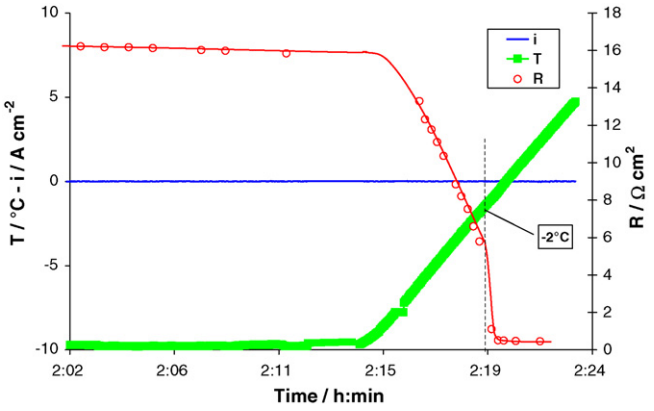

Fig. 10. Time evolution of cell resistance with an imposed warm up after cold start.

same time when the upward temperature reaches −2 °C and the downward −6 °C. This reflects the water phase change. In the first case, ice melts and in the second case water freezes. As explained at the experimental part, the FC temperature is the temperature measurement of coolant fluid at the FC outlet. The maximal coolant temperature difference between inlet/outlet observed at the maximal cold start power is 0.1 °C. Thus, the difference between −2 and −6 °C is attributable to the temperature difference between the coolant fluid and the MEA due to transient ramp. Consequently the water melting/freezing point inside the CCL would rather be about −4 °C.

Fig. 10 presents the cell resistance evolution during an imposed warm up of the FC after it underwent a long cold start. In this experiment the electronic load is disconnected and gas flows are cut off. Pineri et al. [14] indicate that for a fully hydrated membrane inside an airtight glass capillary, the cooling process entails the water desorption of the membrane. Ice crystal formation was observed preferentially on the glass capillary surfaces because of cooler surfaces of the experimental set-up and not on the membrane surface. According to results obtained by Pineri et al., water in persulfonated membrane is at a supercooled state. In this configuration, RH is defined as the saturating vapour pressure over ice in atmosphere (or space) divided by the saturating vapour pressure over supercooled water [16]. Thus, RH of a fully hydrated membrane decreases with temperature below the freezing point and would lead to the decrease of the membrane water content by vapourisation. This vapour condenses during the cooling stage on cold points of the glass capillary. Theoretically, this behaviour is reversible during the heating process (with kinetic not necessarily identical). This is reinforced by Pineri et al. [14] who observed that during reheating, water is reabsorbed into the membrane. Consequently, with the FC temperature increase, ice sublimates and the sublimated vapour is absorbed by the membrane. Thus, ice decrease reduces contact resistances and therefore the cell resistance. When the freezing temperature is reached in the CCL, ice melts and the cell resistance drops suddenly because contact resistances induced by ice disappear. The melting temperature with no current and no gas flow is the same than the one observed for a cold start with an imposed warm up (Fig. 9). Therefore, this result confirms that water melting/freezing point inside the CCL is well around −4 °C.

Results in Fig. 9 also indicate that a FC suffering an important starving can restart if its temperature rises over the melting/freezing point inside the CCL.

3.5. Effect of imposed temperatures

Fig. 11 describes the effect of the cell temperature on potentiostatic cold starts. Under these harsh conditions (imposed temperature), FC can start for temperatures above −5 °C. This temperature is close to ice melting point in the CL of −4 °C, as it has been observed in the temperature ramp tests above. Below −5 °C, performance at subzero temperatures drops quickly. Nevertheless, the cumulated heat density generation calculated with Eq. (1) allows predicting that investigated FC should be able to self-start in less than 30 s for an initial temperature of −10 °C (the heat capacity of a cell including a bipolar plate, a MEA and the coolant is about

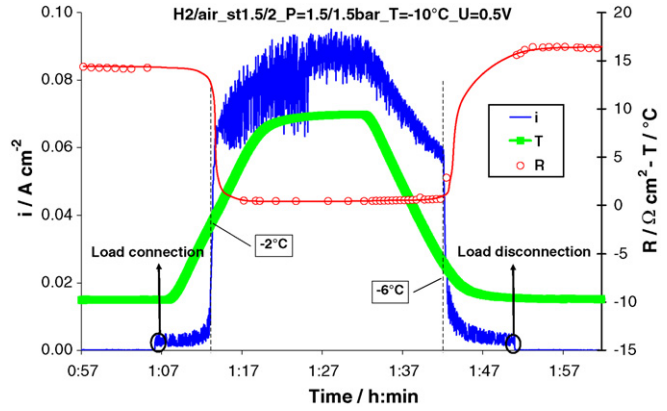

Fig. 9. Time evolution of current and cell resistance during cold start with upward and downward cell temperature ramps.

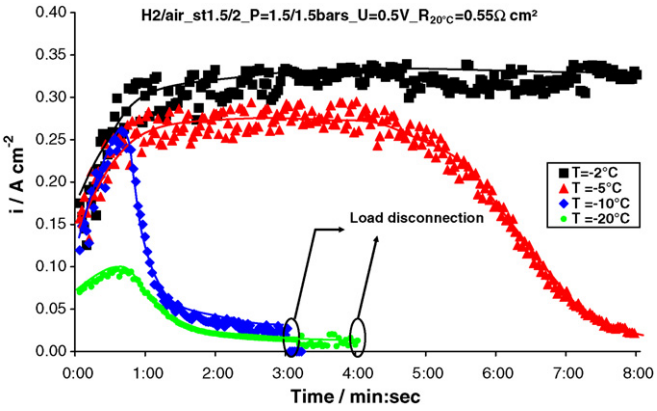

Fig. 11. Time evolution of current density during cold starts at different imposed temperatures.

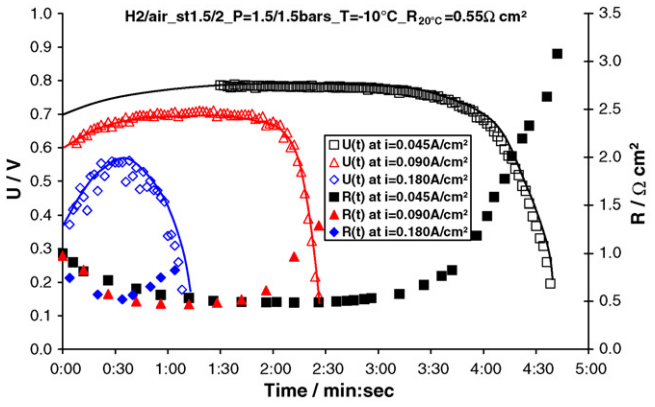

Fig. 12. Time evolution of cell voltage and cell resistance during cold starts at different imposed current densities.

63 J K^{-1}). However, it would not be possible to self-start for a temperature of −20 °C.

3.6. Effect of imposed current densities

Fig. 12 displays the current density effect on galvanostatic cold starts. The general FC behaviour is similar to the one under potentiostatic mode. However, the starving stage is shorter as current density and produced water remain constant. The main interest of test performed in galvanostatic mode is to quantify additional phenomena during starving stage. This is in part possible by the overpotential assessment with the measurements of the current density "i", the cell voltage "$U(t)$" and the ohmic cell resistivity "$R(t)$". Change in ohmic drop "ΔU_Ω" when starving begins at the maximal voltage "U_{max}" and also corresponding to the minimal cell resistivity "$R_{U_{max}}$", can be calculated by

$$\Delta U_\Omega(t) = (R(t) - R_{U_{max}})i \quad (2)$$

Change in electrodes overpotential "$\Delta\eta_{Electrodes}$" (diffusion + activation) when starving begins is evaluated by

$$\Delta\eta_{Electrodes}(t) = (U_{max} - U(t)) - \Delta U_\Omega(t) \quad (3)$$

Time evolution of ΔU_Ω and $\Delta\eta_{Electrodes}$ from Eqs. (2) and (3) is shown in Fig. 13. The part of ohmic drop change in comparison with total overpotential change is

$$\frac{\Delta U_\Omega(t)}{\Delta U_\Omega(t) + \Delta\eta_{Electrodes}(t)} \quad (4)$$

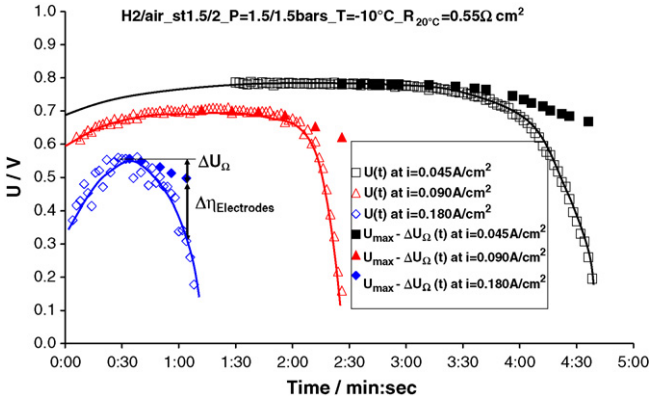

Fig. 13. Time evolution of cell voltage and ohmic drop during starving stage of cold starts at different imposed current densities.

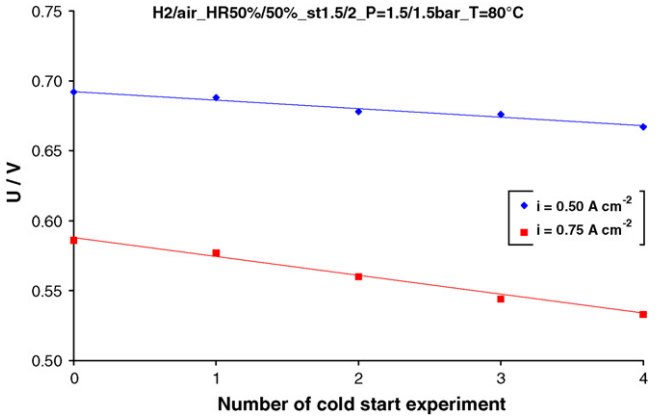

Fig. 14. Evolution of FC performances at rated conditions after each cold start.

At the starving step, the ohmic drop represents about 40% of the total measured overpotential. After, when performances decrease sharply, the electrode overpotential, mainly due to diffusion and activation limitations, becomes higher and higher.

3.7. Ageing

Polarization curves under rated conditions (80 °C) were carried out after each start up at subzero temperatures. FC MEA is changed at the end of each investigated parameter. Therefore, number of tests performed on each MEA is relatively low but allows quantifying the performance degradation tendencies. It is found that performances for cold starts performed at −10 °C reduce less than 1% per cold start at 0.5 A cm^{-2} and about 2% at 0.75 A cm^{-2} (see Fig. 14). Voltage loss accelerates from 0.5 to 0.75 A cm^{-2}. This is characteristic of a gas diffusion limitation towards the catalytic sites. According to the literature, this behaviour can arise from two phenomena:

- MEA layers become more hydrophilic because of PTFE loss and/or structure alterations induced by ice expansion [2]. Hou et al. [9] suggested that the water freezing would compress the pores in agglomerates inducing agglomerates diffusion effects. Whatever it can be, both papers agreed that structure modifications lead to irreversible performance loss.
- A film of water appears after ice melting which plugs the pores [9]. A similar interpretation is proposed by Ge and Wang [8] where water is trapped between particles and ionomer of the CCL as a result of ice melting. What ever it can be, both papers agreed that the residual water leads to reversible performance loss.

4. Conclusions

Ice/frost formation in a PEMFC operating under subzero temperatures can lead to its shutdown during start up. Isothermal potentiostatic and galvanostatic tests were performed on a 220-cm^2 single cells made of thin metallic sheets, under a wide range of operating conditions in order to investigate its "cold start" behaviour. Different parameters have been investigated: the initial water contained in the membrane, the imposed voltage, the cell temperature and the current density.

Results allowed proposing a better cold start understanding:

- FC starving is not only due to ice formation in the cathode layer pores hindering oxygen transport. It is also due to ice formation in active reaction sites increasing the electrical resistance of the cell. Both factors dramatically reduce FC performance under load. The

relative balance of each effect has been assessed. At the beginning of the starving step for a galvanostatic cold start, the ohmic drop represents about 40% of the total measured overpotential. After, when performance decreases sharply, the electrode overpotential, mainly due to diffusion and activation limitations, becomes higher and higher.
- Ice formed inside the CCL does not locate at the same place during the cooling stage and during cold start stage. Ice formed in a wet MEA due to FC cooling without operation would locate only in the hydrophilic pores. During starving phases, ice would not only locate in the pores of the CCL, but also at the interfaces of particle agglomerates of ionic and electronic conductors inside the CCL.

About operating condition influences, following conclusions can be formulated:

- An optimal wetting level appears when the cumulated heat generated by the electrochemical reaction is maximal. This information is useful in order to obtain a maximal heat generation to allow self-starting without additional heat source.
- To take the maximum benefit of the heat generation for self-starting on a duration compatible with automotive application (<30 s), starting at low voltage ($0.3 < U_{cell} < 0.5$ V) is preferable.
- The water melting/freezing point inside the CCL was found to be about −4 °C. A FC suffering an important starving can restart if its temperature rises over this point.
- FC made of thin investigated metallic sheets and previously dried should be able to self-start in less than 30 s, for an initial temperature of −10 °C. However, this would not be possible for a temperature of −20 °C.

Successive cold starts entail an acceleration of the performance drops for current densities in rated conditions (80 °C) higher than 0.5 A cm^{-2}. This is characteristic of a gas diffusion limitation towards the catalytic sites that might be due to structure modifications induced by ice expansion and residual water trapped in the CCL after ice melting.

Acknowledgment

This work was financially supported by the French research agency ANR PAN'H within the framework of the MEPHISTO project.

Appendix A. Relation between cell resistance and water content

The maximum value of water content in the membrane "λ" (ratio of the water molecule to the number of charge sites) is obtained when the water vapour at its interface is saturated. In this case, λ is about 14. When the membrane is in contact with liquid water, Springer et al. [17] report that λ at 80 °C is about 16.8.

The value of λ under saturating conditions depends on the ratio of vapour water and liquid water at the membrane interface. When the FC operates in nominal conditions, the membrane is in an environment of a mixture of saturated vapour and liquid water. In this condition λ can be assessed at the average value of 15. So, the cell resistance measured in this condition with the impedance-meter would correspond to a water content λ of 15. The cell resistance "R_{cell}" includes not only the membrane resistance "R_{memb}" but also the contact and the cell material resistances. Specific measurements were performed to determine the resistance of the GDL pressed between tow bipolar plates. This value is about 0.044 Ω cm^2 for positive temperature. Thus, R_{memb} can be assessed from the R_{cell} measurement by

$$R_{memb} = R_{cell} - 0.044 \quad (A.5)$$

R_{memb} is generally estimate by the following equation:

$$R_{memb} = \frac{t_{memb}}{\sigma_{memb}} \quad (A.6)$$

where "t_{memb}" is the membrane thickness and "σ_{memb}" the proton conductivity of the membrane. The commonly equation used to calculate σ_{memb} is the one of Springer et al. [17] for 117 NAFION®, at which one is added a coefficient "C" by Poirot [18] to take into account other types of polymer membrane:

$$\sigma_{memb} = C(33.75\,\lambda - 21.41)\,\exp^{(-1268/T)} \quad (A.7)$$

"T" is the temperature in Kelvin. This formulation is validated with temperature from 30 to 80 °C and for λ > 1. According to Ahluwalia and Wang [19], this relation can be applied up to −15 °C for λ = 14 and up to −30 °C for λ = 3. R_{cell} measured under operating nominal conditions at 80 °C is 0.132 Ω cm^2. Eq. (A.5) gives R_{memb} = 0.088 Ω cm^2. As explained previously, λ is supposed to be around 15 under these conditions. Thus, the value of C for the investigated membrane used in the MEA is evaluated by solving of Eq. (A.7):

$$C = 0.22 \quad (A.8)$$

Eq. (A.7) indicates that, for a constant water content and whatever its value, R_{memb} rises by a 2 factor from 80 to 20 °C and by a 1.6 factor from 20 to −10 °C. R_{memb} deduced from Eq. (A.5) and from the experimental cell resistances measured until step 6 of the testing procedure are in good agreements with these factors. It has to be nevertheless noted that this model has not been experimentally validated with specific measurements of R_{memb}(λ, T).

For a known temperature and a known cell resistance, Eqs. (A.5)–(A.8) allow to estimate the water content of the membrane. Table 1 shows λ versus R_{cell} calculated from the model at the drying temperature of 20 °C.

Table 1
Expected water content of the membrane at the drying temperature of 20 °C vs. cell resistances.

$R_{cell20\,°C}$ (Ω cm^2)	λ
0.22	15
0.37	8.3
0.55	5.7
0.92	3.5
1.58	2.3

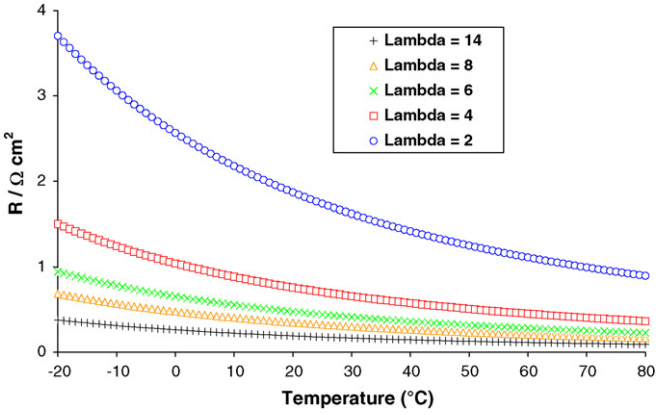

Fig. 15. Expected membrane resistance as a function of temperature and water content.

Fig. 15 displays the expected membrane resistance from the model as a function of temperature and water content.

References

[1] Y. Hishinuma, T. Chikashisa, F. Kagami, T. Ogawa, JSME Int. J. B 47 (2004) 235–241.
[2] M. Oszcipok, D. Riemann, U. Kronenwett, M. Kreideweis, M. Zedda, J. Power Sources 145 (2005) 407–415.
[3] M. Oszcipok, M. Zedda, D. Riemann, D. Geckeler, J. Power Sources 154 (2006) 404–411.
[4] Q. Yan, H. Toghiani, Y.W. Lee, et al., J. Power Sources 160 (2006) 1242–1250.
[5] K. Tajiri, Y. Tabuchi, F. Kagami, et al., J. Power Sources 165 (2007) 279–286.
[6] K. Tajiri, Y. Tabuchi, C.Y. Wang, J. Electrochem. Soc. 154 (2007) B1147–B1152.
[7] S. Ge, C.Y. Wang, Electrochem. Acta 52 (2007) 4825–4835.
[8] S. Ge, C.Y. Wang, J. Electrochem. Soc. 154 (2007) B1399–B1406.
[9] J. Hou, W. Song, H. Yu, Y. Fu, Z. Shao, B. Yi, J. Power Sources 171 (2007) 610–617.
[10] E. Cho, J.J. Ko, H.Y. Ha, S.A. Hong, K.Y. Lee, T.W. Lim, I.H. Oh, J. Electrochem. Soc. 150 (2003) A1667–A1670.
[11] S. Kim, M.M. Mench, J. Power Sources 174 (2007) 206–220.
[12] J. Hou, H. Yu, S. Zhang, S. Suna, H. Wang, B. Yi, P. Minga, J. Power Sources 162 (2006) 513–520.
[13] Q. Guo, Z. Qi, J. Power Sources 160 (2006) 1269–1274.
[14] M. Pineri, G. Gebel, R.J. Davies, O. Diat, J. Power Sources 172 (2007) 587–596.
[15] M. Oszcipok, A. Hakenjos, D. Riemann, C. Hebling, Fuel Cells 7 (2007) 135–141.
[16] http://www.natmus.dk/cons/tp/cool/suprcool.htm, Copyright: Tim Padfield, May 1999.
[17] T.E. Springer, T.A. Zawodzinski, S. Gottesfeld, J. Electrochem. Soc. 138 (1991) 2334–2342.
[18] J.P. Poirot, Thesis, Institut National Polytechnique de Grenoble, 2000.
[19] R.K. Ahluwalia, X. Wang, J. Power Sources 162 (2006) 502–512.